Optics Letters

Auto-pump-depleted stable single-longitudinal-mode 1.5 μm source with the assistance of SHG

Xiaobin Peng,[1] Lichao Duan,[1] Jiao Wei,[1,2] Jing Su,[1,2] Huadong Lu,[1,2,*] and Kunchi Peng[1,2]

[1]State Key Laboratory of Quantum Optics and Quantum Optics Devices, Institute of Opto-Electronics, Shanxi University, Taiyuan 030006, China
[2]Collaborative Innovation Center of Extreme Optics, Shanxi University, Taiyuan 030006, China
*luhuadong@sxu.edu.cn

Received 31 August 2023; revised 6 October 2023; accepted 6 October 2023; posted 6 October 2023; published 25 October 2023

To realize a stable single-longitudinal-mode (SLM) 1550-nm light source for the generation of non-classical states, a ring auto-pump-depleted singly resonant optical parametric oscillator (SRO) with the assistance of second-harmonic-wave generation (SHG) is designed and built in this Letter. A magnesium oxide doped periodically polarized lithium niobate (MgO:PPLN) crystal and a lithium triborate (LBO) crystal are employed as the optical parametric downconversion (OPDC) and SHG crystals, respectively. Especially, the introduced SHG can firstly increase the loss difference between the lasing and non-lasing modes so that the dual-mode or multi-mode coupling in the achieved SRO can be effectively eliminated and the stable SLM operation is achieved. At the same time, the SHG will automatically adjust the output coupling efficiency of SRO, so as to achieve efficient conversion efficiency and auto-pump depletion of SRO. In addition, due to the SHG, it is easy to achieve the low-intensity noise multi-wavelength output for the stable SLM SRO. As a result, the output powers of the SLM 1550 nm and 775 nm are up to 4.05 W and 3.25 W, respectively, and the total optical conversion of the built SRO can achieve 45.58%. The presented method paves a way to develop a compact stable SLM multi-wavelength SRO, and the obtained SRO is further beneficial to develop compact continuous-variable non-classical light fields. © 2023 Optica Publishing Group

https://doi.org/10.1364/OL.504518

Continuous-variable (CV) quantum light sources are important non-classical light sources and have been applied in lots of fields, such as quantum teleportation, quantum key distribution, quantum computation, and so on, because of their intrinsic advantages in the intensity noise lower than the quantum noise limit (QNL). Especially, in order to establish quantum light sources matching with the optical fiber communication, it is urgent to develop a stable single-longitudinal-mode (SLM) continuous-wave (CW) 1.5 μm light source with high power and low noise. So far, the 1.5 μm laser can be directly generated by GaAs and GaInAs semiconductor laser [1], all-solid-state Er:Yb:YAB laser [2], as well as erbium-doped fiber laser [3]. However, compared to the above methods, an optical parametric oscillator (OPO) has been attracting wide attentions due to its advantages of high power, wide tuning, narrow linewidth, low noise, and so on [4]. As early as 1969, Kreuzer had given a theoretical treatment of the SRO and showed that in steady-state operation, the gain saturation would prevent more than one mode from oscillating if the pump power is less than 4.6 times threshold [5]. In other words, when the output power of OPO was increased by increasing the incident pump power, frequent mode-hopping and multi-longitudinal-mode (MLM) phenomena [6] due to the gain saturation mechanism were easily observed. Therefore, an etalon is often inserted into the OPO resonator [7] to increase the loss of the non-lasing modes. However, the inserted loss caused by the etalon simultaneously increases the intra-cavity loss and further restricts the output power of the main lasing mode. Additionally, in order to maintain the stable SLM operation of the OPO in the case of considering the length variation of the OPO resonator and the frequency drift of the pump source, the transmission peak of the adopted etalon has to be locked with the oscillating longitudinal mode of the OPO resonator, which cannot be conducive to miniaturization of the OPO. In 1997, an effective method for suppressing MLM oscillation and mode hopping in a solid-state resonator was developed by Martin *et al.* [8], which was implemented by introducing a nonlinear loss into the resonator to increase the nonlinear loss difference between the lasing and non-lasing modes. Later, our group not only proposed a physical condition of SLM operation for a high-power laser based on the nonlinear loss but also improved the overall performance of the laser depending on the nonlinear loss including effectively decreasing the intensity noise, precisely measuring the intra-cavity linear loss, improving the power and frequency stability, expanding the continuous frequency-tuning rang and so on [9]. Although the intracavity-frequency-doubled OPOs have been broadly studied, the effects of the intracavity second-harmonic-wave generation (SHG) on the longitudinal stability and the auto-adjustment of the pump depletion and extraction conversion efficiency are not reported, to the best of our knowledge.

Therefore, we presented a new method to realize a compact and stable SLM SRO with the assistance of the nonlinear loss by introducing SHG in this Letter. Owing to the SHG, the loss difference between the lasing and non-lasing modes was increased,

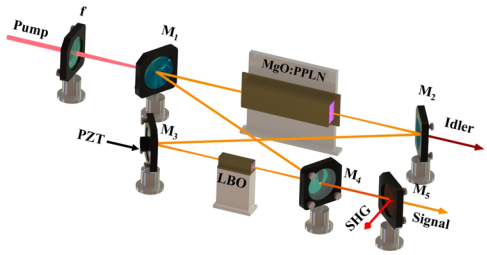

Fig. 1. Schematic diagram of the designed SRO.

and the multi-mode coupling and mode hopping were effectively suppressed. Especially, the output coupling efficiency of OPO can be automatically adjusted, which is beneficial for achieving the high pump depletion. At the same time, the multi-wavelength and the low-intensity noise output were achieved.

The schematic diagram of the designed and built OPO with the intra-cavity SHG is described in Fig. 1. The presented OPO is a single resonant optical parametric oscillator (SRO) for signal light. The pump source is a homemade all-solid-state single-frequency CW 1064 nm laser (DPSS FG-VIII, Yuguang Co., Ltd.), whose long-term power stability and beam quality factors M^2 are better than ±1.00% and 1.10, respectively. The polarization direction of the 1064 nm laser is firstly aligned by a halfwave-plate in front of the SRO resonator. After, the waist radius of 1064 nm laser is focused to 60.75 μm by a focusing lens of f=120 mm to realize precise quasi-phase matching (QPM), and the laser is injected into the SRO resonator. To achieve efficient tri-wavelength outputs, a compact SRO resonator with double-cavity-mode waists is designed and built, which is composed of four concave mirrors (M_1, M_2, M_3, M_4). The input coupler M_1 is a concave–convex mirror with the curvature radius of 60 mm, and both surface is antireflection (AR) films coated (T=99.50%) for 1064 nm and 3050–3800 nm, and high reflection (HR) films (R=99.50%) for 1490–1620 nm. M_2 is a plane–concave mirror with the curvature radius of 60 mm and both surface is AR films coated (T=99.50%) for 1064 nm and 3050–3800 nm and HR films coated (R=99.50%) for 1490–1620 nm. Both M_3 and output coupler (OC) M_4 are plane–concave mirror with the curvature radius of 40 mm. The M_3 surface is HR films coated (R=99.50%) for 1490–1620 nm and M_4 surface is partial transmission films coated (T=1.00%) for 1490–1620 nm and HT films coated for 730–850 nm. To convert the incident pump laser into the signal and idler light as high as possible, a periodically polarized lithium niobate crystal doped with the magnesium oxide of 5% (MgO:PPLN) is selected to act as the optical parametric downconversion (OPDC) medium for QPM owing to its intrinsic advantages of low absorption loss, high nonlinear coefficient, and high resistance to photorefractive effect. Its cross section and length are 1×10 mm^2 and 40 mm, respectively, and it is placed at the beam waist between M_1 and M_2. Both end-faces of the crystal are AR films for 1064, 1400–1800, and 2600–4800 nm. To introduce enough nonlinear loss, a high optical damage threshold lithium triborate (LBO) crystal for type I critical phase matching with the dimensions of 2×2×12 mm^3 is employed as the SHG medium and placed at the beam waist between M_3 and M_4 for achieving efficient SHG. Both end-faces are AR films for 1400–1800 and 730–850 nm. The piezoelectric transducer (PZT) is used to lock the OPO to a high-fine hyper-stable cavity. In the experiment, the radii of the cavity mode beam waists in the MgO:PPLN and LBO crystal are 73.36 and 56.76 μm, respectively. Both the MgO:PPLN and LBO crystal are placed in copper ovens whose temperatures are precisely controlled by a high precision temperature controller (YG-4S, Yuguang Co., Ltd.) with a temperature control accuracy of 0.01 °C, respectively. In this case, the residual pump and idler output from M_2. The signal and second-harmonic-wave light leak from M_4, and they are further separated by another dichroic mirror M_5 for recording their output power.

When only the MgO:PPLN crystal is inserted into the SRO resonator, the intra-cavity signal power and the optical conversion efficiency of the signal light are evaluated by [10]

$$P_s = \frac{\lambda_p}{\lambda_s}\left[\frac{12(k-1)(1+2m)}{(1+m)C\xi_s} - \frac{24(k-1)^2(2+4m)\varepsilon}{C^2\xi_s^2 P_p}\right], \quad (1)$$

$$\eta_s = \frac{P_{s,out}}{P_p} = \frac{P_s T_s}{P_p}, \quad (2)$$

where λ_p, λ_s, and λ_i are the wavelengths of the pump, signal and idler light; m is the overlap degree of pump and signal beams; ξ_s is the focusing factor; k is the wave vector ratio; P_p is the incident pump power; ε is the total loss, $\varepsilon = T_s + V$, where T_s and V are the transmission of OC for the signal light and intra-cavity loss, respectively; and C is constant about the MgO:PPLN crystal parameters.

Once the LBO crystal is inserted into the SRO resonator, the intra-cavity signal power is updated as

$$P'_s = \frac{\lambda_p}{\lambda_s}\left[\frac{12(k-1)(1+2m)}{(1+m)C\xi_s} - \frac{24(k-1)^2(2+4m)\varepsilon'}{C^2\xi_s^2 P_p}\right]. \quad (3)$$

Due to the introduction of nonlinear loss ε_{SHG}, intra-cavity loss will be changed to V', respectively. The total loss is defined, $\varepsilon' = T_s + V' + \varepsilon_{SHG}$, and ε_{SHG} is written as [11]

$$\varepsilon_{SHG} = \frac{8\pi^2 l_{lbo}^2 d_{lbo}^2}{(n'_s)^2 n_{sh}\lambda_s^2 c\varepsilon_0}\frac{P'_s}{\pi\omega_s^2}, \quad (4)$$

where d_{lbo} and l_{lbo} are the effective nonlinear coefficient and length of LBO crystal, respectively; n'_s and n_{sh} are the index refraction of LBO crystal for the signal and second-harmonic-wave light; and ω_s is the waist radius of a signal beam in the LBO crystal.

So, the total conversion efficiency of the signal and second-harmonic-wave light is refreshed as

$$\eta_{s+SHG} = \frac{P_{s,out} + P_{SHG}}{P_p} = \frac{P'_s T_s + P'_s \varepsilon_{SHG}}{P_P}. \quad (5)$$

According to Eqs. (2) and (5), the optical conversion efficiency with variation of the transmission of OC before and after inserting the LBO crystal at the maximum incident pump power of 24.60 W are depicted in Fig. 2. It is clear that the optimal transmission of OC for the signal light is 2.43% before inserting the LBO crystal, which means that the transmission of 1.00% adopted in the experiment is so small that other longitudinal modes can easily reach the oscillating threshold and begin to oscillate together with the main longitudinal mode. In this case, the dual-mode and multi-mode coupling will be easily observed, and the SRO will work with MLM or mode-hopping operation. Once the LBO crystal is inserted into the resonator, the nonlinear loss difference between the lasing and non-lasing modes is increased. In this case, the oscillating threshold values for the non-lasing modes are too high to reach. As a result, the non-lasing modes can be effectively suppressed, and the SLM

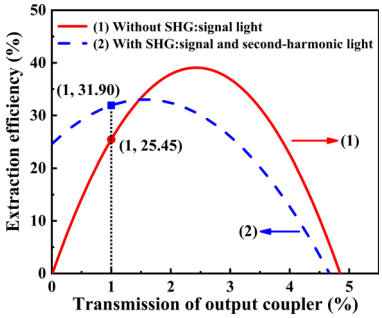

Fig. 2. Theoretical prediction of the optical conversion efficiency versus transmission of OC at the incident pump power of 24.60 W.

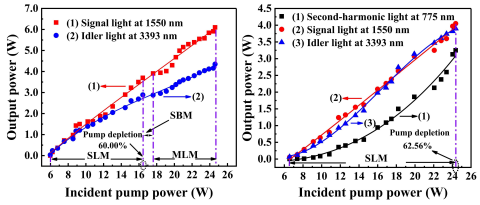

Fig. 3. Output power versus the incident pump power. (a) Without SHG. (b) With SHG.

operation for the built SRO is attained. It can also be clearly seen from Fig. 2 that when the transmission of the output coupling mirror is too small, more fundamental-wave signal will be converted into second harmonic wave and leak from the output coupling mirror. However, when the transmission of the OC is large enough, the fundamental-wave signal light is directly output from the output coupling mirror, and SHG efficiency will be very small at this time. In other words, the SHG can simultaneously automatically manipulate the output coupling for the signal light and make the OPO achieve efficient conversion efficiency as high as possible, which is also conducive for the OPO to achieve stable SLM operation and high pump depletion.

In the experiment, when the grating period and the temperature of the adopted MgO:PPLN crystal were Λ =30.49 μm and 46.82 °C, the wavelengths of the signal and idler light were adjusted to 1550 and 3393 nm, respectively. Firstly, the output power with the increase of the incident pump power is recorded before and after the LBO crystal was inserted into the SRO resonator, which are shown in Fig. 3. Before the LBO crystal was inserted into the SRO resonator, according to Fig. 3(a), the measured threshold pump power was 6.00 W, and the maximum output powers of the signal and idler light were 6.10 and 4.30 W at the incident pump power of 24.60 W, respectively. Only considering the signal light, the optical conversion efficiency was 24.80%. When the LBO crystal was inserted into the SRO resonator and the SRO resonator was realigned, the obtained threshold pump power was 6.50 W. In this case, the temperature of the CPM-LBO crystal was controlled at 25 °C to achieve the maximum efficiency output. The measured maximum output powers of signal and idler light were 4.05 and 3.90 W at the same incident pump power of 24.60 W, respectively. At the same time, a second-harmonic-wave 775 nm beam with the output power of 3.25 W was also attained, which is depicted in Fig. 3(b). It could be seen that the conversion efficiency from the incident pump laser to the signal and second-harmonic-wave light was

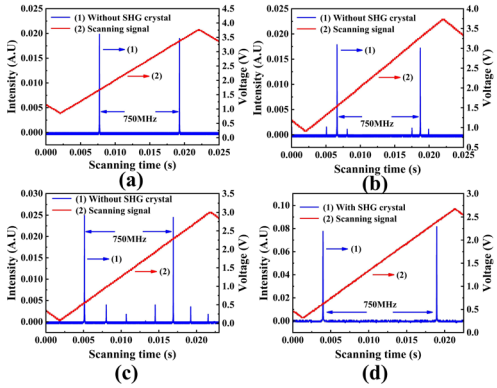

Fig. 4. Longitudinal-mode structures of the signal light. (a) <16.50 W, without SHG. (b) From 16.50 to 17.60 W, without SHG. (c) >17.60 W, without SHG. (d) With SHG.

29.67%, which was higher than 24.80% without the SHG. Considering the idle light, the overall optical conversion efficiency of the SRO was increased from 42.28% to 45.53% after introducing the SHG. From Fig. 3, we could conclude that extraction efficiency had obvious improvement after the introduction of the nonlinear loss at the same transmission of the output coupler. The experimental results were in good agreement with the previous theoretical predictions.

In the process of recording the output powers of the designed SRO before and after inserting the LBO crystal, the longitudinal-mode structures were simultaneously monitored by employing a F–P interferometer with the free spectrum range of 750 MHz and finesse of 120, and the monitored results are illustrated in Fig. 4. The longitudinal-mode structures of the designed SRO at different incident pump power intervals are marked in Fig. 3. Before the LBO crystal was inserted into the SRO resonator, the SRO could work well with SLM operation when the incident pump power was below 16.50 W, which is shown in Fig. 4(a). But, when the incident pump power was increased between 16.50 and 17.60 W, a pair of sideband modes were stimulated, which is shown in Fig. 4(b). When the incident pump power was higher than 17.60 W, the SRO worked with MLM operation, which is shown in Fig. 4(c). By contrast, once the SHG was introduced into the resonator, the stable SLM operation was obtained for the SRO from the threshold incident pump power to the maximum value, which is displayed in Fig. 4(d). From Figs. 3 and 4, we also found that the MLM operation began at 2.75 times of the threshold incident pump power when the SHG was not introduced. On the contrary, after the SHG was introduced to the resonator, the designed SRO still maintained the SLM operation despite the incident pump power of 3.78 times of the threshold value. In addition, the numerical values of pump depletion were measured at the SLM operation. The values of pump depletion were increased from 60.00% to 62.56% at the SLM operation before and after the introduction of the SHG process, which are also marked in Figs. 3(a) and 3(b). It also means that the introduced nonlinear loss not only improve the stable SLM operation but also achieve a high pump depletion at the SLM operation range. Moreover, it was easy to be observed that the environment adaptivity of the achieved SRO was effectively enhanced because the mode hopping could not happen in the experiment although the pump source had an occasional mode-hopping or MLM phenomenon.

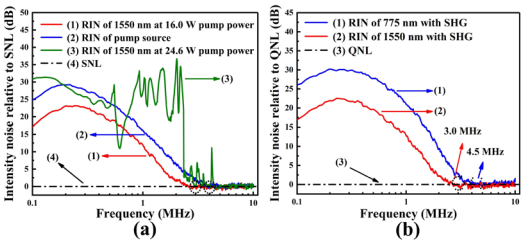

Fig. 5. RIN spectra, (a) Without SHG, (b) With SHG.

In addition, the intensity noise of the output light was experimentally studied before and after introducing the SHG into the build SRO. The intensity noise was measured by employing a homemade balanced homodyne detector (BHD01, Yuguang Co., Ltd.), and the measured results are shown in Fig. 5. Curves (1), (2), and (3) in Fig. 5(a) were the measured intensity noise spectra of the 1550 nm light relative to the shot noise level (SNL) for the incident pump power of 16.00 W (SLM) and 24.60 W (MLM) as well as the incident pump laser, respectively. It was clear that the intensity noise of the 1550 nm signal light reached the SNL at the frequency of 3.00 MHz when the SRO worked with the SLM operation, which is lower than that of the incident pump laser of 4.00 MHz. Moreover, the relaxation oscillation (RRO) peaks were not observed for the incident pump laser and the signal 1550 nm light, which was ascribed to the RRO suppression of the incident pump source depending on the nonlinear loss [12]. However, the intensity noise of 1550 nm was obviously increased for the whole analyzed frequencies when the SRO worked with the MLM operation, which depicted that the coupling between different longitudinal modes could increase the intensity noise of the obtained SRO. Figure 5(b) illustrated the intensity noise spectra of the 1550 nm and 775 nm at the highest incident pump power of 24.60 W after the SHG was introduced in the resonator. It could be found that the MLM could be successfully suppressed, and the intensity noise of the 1550 nm and 775 nm reached the SNL at the frequency of 3.00 and 4.50 MHz, respectively. From Fig. 5, it was found that the nonlinear loss introduced by SHG was beneficial for attaining a low-intensity noise OPO with high output power except for achieving the SLM operation and auto-pump depletion for the OPO. On this basis, the long-term power stabilities of the 1550 and 775 nm during 5 h were measured, and the power stabilities of the 1550, 775, and 3393 nm were better than ±1.10%, ±1.20%, and ±1.10%, respectively, which were depicted in Fig. 6(a). The beam quality factors M^2 of the 1550 nm and 775 nm were also measured using a M^2 beam quality analyzer (M^2SETVIS, Thorlabs) at the maximum output power. The spatial beam profiles and corresponding caustic curves are shown in Figs. 6(b) and 6(c). It could be seen that the measured M^2 factors were better than 1.07 and 1.05 in x and y directions for 1550 and 775 nm, respectively. Moreover, due to the spatial walk-off effect of type I critical phase-matching LBO crystal, the elliptic beam profile of 775 nm was easily seen from the inset of the Fig. 6(c).

In conclusion, we presented a compact and stable SLM SRO with high power tri-wavelength of 1550 nm, 3393 nm, and 775 nm, which was achieved by combining OPDC with SHG in a resonator. The introduction of the nonlinear loss could not only suppress the MLM and mode-hopping phenomena but also automatically adjust the output coupling efficiency of the built SRO. It is easy to achieve efficient conversion efficiency and

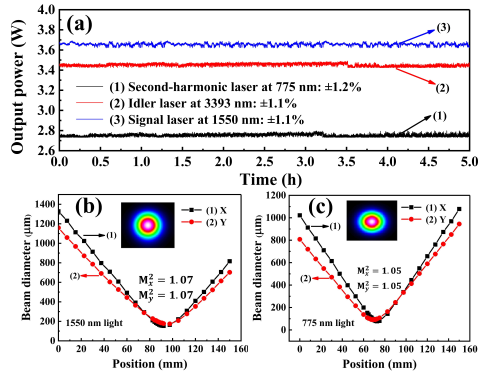

Fig. 6. Measured output performances, (a) Power fluctuations of the output, (b) transverse-mode characteristic of the signal light. (c) Transverse-mode characteristic of the SHG light.

high pump depletion as high as possible as well as realize the low-ntensity noise output. As a result, the maximum output powers of the signal 1550 nm, idler 3393 nm, and second harmonic wave 775 nm were up to 4.05, 3.90m and 3.25 W, respectively, and the total optical conversion efficiency was up to 45.58%. The beam quality factors M^2 of the signal and second–harmonic–wave lights were greater than 1.07 and 1.05, and the peak-to-peak power stabilities of the second harmonic wave, signal, and idler lights were better than ±1.20%, ±1.10%, and ±1.10%. The attained compact high-power SLM tri-wavelength SRO with low-intensity noise is beneficial to develop a compact CV non-classical quantum light source.

Funding. National Natural Science Foundation of China (61975100, 62105192, 62205186, 62027821); National Key Research and Development Program of China (2022YFC2204003); Applied Basic Research Project of Shanxi Province, China (202103021221004, 202203021212478); Fund for Shanxi "1331 project" Key Subjects Construction; Research Project Supported by Shanxi Scholarship Council of China (2022-015); Special Fund Project for Science and Technology Innovation Teams of Shanxi Provience (202204051002005); Shanxi Province Patent Conversion Project (202305007).

Disclosures. The authors declare no conflicts of interest.

Data availability. Data underlying the results presented in this Letter are not publicly available at this time but may be obtained from the authors upon reasonable request.

REFERENCES

1. S. Bank, W. Ha, V. Gambin, M. Wistey, H. Yuen, L. Goddard, S. Kim, and J. S. Harris, J. Cryst. Growth **251**, 367 (2003).
2. Y. Chen, Q. Hou, Y. Huang, Y. Lin, J. Huang, X. Gong, Z. Luo, Z. Lin, and Y. Huang, Opt. Express **25**, 19320 (2017).
3. G. Sobon, D. Sliwinska, K. M. Abramski, and P. Kaczmarek, Laser Phys. Lett. **11**, 025103 (2014).
4. K. Devi, S. C. Kumar, and M. Ebrahim-Zadeh, Opt. Lett. **37**, 5049 (2012).
5. L. B. Kreuzer, Appl. Phys. Lett. **15**, 263 (1969).
6. M. Vainio, J. Peltola, S. Persijn, F. J. M. Harren, and L. Halonen, Appl. Phys. B **94**, 411 (2009).
7. X. Hong, X. Shen, M. Gong, and F. Wang, Opt. Lett. **37**, 4982 (2012).
8. K. I. Martin, W. A. Clarkson, and D. C. Hanna, Opt. Lett. **22**, 375 (1997).
9. H. Lu, J. Su, Y. Zheng, and K. Peng, Opt. Lett. **39**, 1117 (2014).
10. S. Guha, Appl. Phys. B **66**, 663 (1998).
11. R. Smith, IEEE J. Quantum. Electron. **6**, 215 (1970).
12. H. Lu, Y. Guo, and K. Peng, Opt. Lett. **40**, 5196 (2015).